SI ADVANCES IN PHOTOSYNTHESIS

Photosynthesis in the fleeting shadows: an overlooked opportunity for increasing crop productivity?

Yu Wang[1] iD, Steven J. Burgess[1] iD, Elsa M. de Becker[1,2] iD and Stephen P. Long[1,3,4,]* iD

[1]*Carl R Woese Institute for Genomic Biology, University of Illinois at Urbana-Champaign, Urbana, IL 61801, USA,*
[2]*Department of Plant Biology, University of Illinois at Urbana-Champaign, Urbana, IL 61801, USA,*
[3]*Department of Crop Sciences, University of Illinois at Urbana-Champaign, Urbana, IL 61801, USA, and*
[4]*Lancaster Environment Centre, Lancaster University, Lancaster LA1 4YQ, UK*

SUMMARY

Photosynthesis measurements are traditionally taken under steady-state conditions; however, leaves in crop fields experience frequent fluctuations in light and take time to respond. This slow response reduces the efficiency of carbon assimilation. Transitions from low to high light require photosynthetic induction, including the activation of Rubisco and the opening of stomata, whereas transitions from high to low light require the relaxation of dissipative energy processes, collectively known as non-photochemical quenching (NPQ). Previous attempts to assess the impact of these delays on net carbon assimilation have used simplified models of crop canopies, limiting the accuracy of predictions. Here, we use ray tracing to predict the spatial and temporal dynamics of lighting for a rendered mature *Glycine max* (soybean) canopy to review the relative importance of these delays on net cumulative assimilation over the course of both a sunny and a cloudy summer day. Combined limitations result in a 13% reduction in crop carbon assimilation on both sunny and cloudy days, with induction being more important on cloudy than on sunny days. Genetic variation in NPQ relaxation rates and photosynthetic induction in parental lines of a soybean nested association mapping (NAM) population was assessed. Short-term NPQ relaxation (<30 min) showed little variation across the NAM lines, but substantial variation was found in the speeds of photosynthetic induction, attributable to Rubisco activation. Over the course of a sunny and an intermittently cloudy day these would translate to substantial differences in total crop carbon assimilation. These findings suggest an unexplored potential for breeding improved photosynthetic potential in our major crops.

Keywords: photosynthetic induction, non-photochemical quenching, NPQ, food security, soybean, wheat, photosystem II, photoinhibition, stomata, crop breeding, leaf canopy, Rubisco activase.

INTRODUCTION

The improvement of crop photosynthesis for yield increases has focused on rates of leaf CO_2 uptake at light saturation (A_{sat}) and under constant light. No correlation between variation in A_{sat} and yield has been found across a selection of modern *Triticum aestivum* (wheat) accessions (Rawson *et al.*, 1983). Furthermore, wild ancestors of wheat showed higher A_{sat} values than elite cultivars (Dunstone *et al.*, 1973). Such influential early findings led to skepticism that photosynthesis can be improved in crops, and this view persists for some today, despite evidence that bioengineered increases in steady-state photosynthesis do

correspond to significant increases in productivity (Köhler *et al.*, 2016; Sinclair *et al.*, 2019; South *et al.*, 2019). Under field conditions, however, the light in a crop canopy is rarely constant. Fluctuations result from intermittent cloud cover but more importantly from the continuous change in the angle of the sun over the course of the day, causing intermittent shadowing within the canopy by overlying leaves and other plant structures (Zhu *et al.*, 2004; Wang *et al.*, 2017b). Might we have overlooked a major opportunity by focusing on steady-state photosynthesis?

A dynamic light environment affects photosynthesis in two main ways. First, a leaf in the shade of another

receives about 1/10th of the light of a leaf in full sun (Zhu *et al.*, 2004). These periods of full sun and of shade may last from seconds to hours (Zhu *et al.*, 2004; Deans *et al.*, 2019; Tanaka *et al.*, 2019). Using reverse ray tracing, and assuming a random distribution of leaves, Zhu *et al.* (2004) showed that even on a clear day, leaves in a static canopy will experience over 20 sun–shade–sun transitions. When leaves move into full light after a period of shade, the leaf CO_2 uptake rate (A) does not instantly reach its maximum value, but rises gradually over several minutes to approach a new steady state. This has been termed photosynthetic induction, and it causes a substantial reduction in the efficiency of carbon fixation (Yamori *et al.*, 2012; Soleh *et al.*, 2017; Taylor and Long, 2017; Salter *et al.*, 2019). Second, leaves in full sunlight receive more energy than they can use, leading to the activation of non-photochemical quenching (NPQ), which dissipates excess energy as heat. This reduces the production of oxidizing radicals via excited-state chlorophyll molecules that would damage the photosynthetic apparatus. Similarly, in a sun–shade transition there is a loss of potential CO_2 assimilation. This is because various components of NPQ have relaxation half-lives ranging from seconds to hours, and therefore the leaf continues dissipating light as heat even after it is moved into the shade, where it could use all of the light received in photosynthesis. This forces A below the steady-state level that it will eventually resume. Practical proof of the importance of this was shown with a bioengineered increase in the rate of dissipation of NPQ during sun–shade transitions. This resulted in a doubling of A in fluctuating light and a significant increase in *Nicotiana tabacum* (tobacco) productivity in replicated-plot field trials (Kromdijk *et al.*, 2016). Many NPQ components have been identified so far, such as: energy-dependent quenching, qE (Krause *et al.*, 1982); zeaxanthin-dependent quenching, qZ (Dall'Osto *et al.*, 2005; Nilkens *et al.*, 2010); chloroplast relocation-dependent quenching, qR (Cazzaniga *et al.*, 2013); state transition-dependent quenching, qT (Nilkens *et al.*, 2010); photoinhibition quenching qI; and photoinhibition-independent sustained quenching qH (Malnoe *et al.*, 2018). However, the relative contribution of these processes may depend on the conditions and species.

It has been argued that evolution and breeder selection would have already optimized photosynthesis in our crops (Winer, 2019). Two factors, with respect to photosynthesis in fluctuating light, counter this argument. First, the ancestors of our major crops evolved in relatively open habitats that could support the production of few leaves, hence both shading and self-shading would have been rare. For example, in the case of *Glycine max* (soybean), the wild ancestor is an annual twining vine that climbs on other stems and spaces its leaves to largely avoid shading. In contrast, modern elite cultivars have been bred as bush forms, grown at densities where they will form 5–7 m^2 of leaf area over every 1 m^2 of field. In essence, the leaves of what were sun plants by origin are now grown so that most leaves are shaded or intermittently shaded. Given the speed at which planting density has increased for our major crops, there is good reason to expect that neither evolution nor breeder selection have kept pace. Indeed, two major crops have now been shown to fail to adapt to shading to optimize canopy photosynthesis (Pignon *et al.*, 2017). Second, current [CO_2] and light levels are co-limiting to photosynthesis in C3 crops. Atmospheric [CO_2] has risen from the 220 ppm average of the past 25 million years to 407 ppm in 2018, with half of that increase occurring in just the last 60 years. This means that light has become progressively more limiting and CO_2 has become progressively less limiting, strongly affecting photosynthetic efficiency in the shade (Long *et al.*, 2004). Again, it is unlikely that there has been sufficient time for any adaptation to this change. This may be reflected in the large variation in speeds of induction on shade–sun transitions within the germplasm of *Manihot esculenta* (cassava), *Oryza sativa* (rice), soybean and wheat (Soleh *et al.*, 2017; De Souza *et al.*, 2019; Salter *et al.*, 2019; Acevedo-Siaca *et al.*, 2020). For example, the between-accession variation in CO_2 assimilated during the induction was three times that of the steady-state assimilation in cassava (De Souza *et al.*, 2019), suggesting that optimization of photosynthesis in fluctuating light has not occurred.

As a result of fluctuations in light the leaf transiently forgoes potential assimilation compared with what could be achieved with an instantaneous response of photosynthesis (Zhu *et al.*, 2004; Taylor and Long, 2017; Deans *et al.*, 2019). Over the course of a day, how much potential photosynthesis does a crop canopy forgo? Two recent estimates predicted a daily loss for wheat of up to 15–21% (Taylor and Long, 2017; Salter *et al.*, 2019); however, these estimates did not use realistic canopy models, simulated only small parts of the canopy and did not consider the combined effect of shade–sun and sun–shade transitions. More accurate assessments of these efficiency losses during light fluctuations require the representation of actual crops and the spatial and temporal dynamics of lighting across all leaves in the canopy.

Using soybean as an example, here the structure of an actual canopy of an elite cultivar is combined with forward ray tracing to predict the spatial dynamics of lighting across the entire canopy throughout the course of both a clear sky and an intermittently cloudy day. This dynamic lighting is combined with kinetics of both induction of photosynthesis and NPQ relaxation to quantitatively review the losses that result compared with an instantaneous return to steady-state photosynthetic rates on light transitions. To simplify the simulation, we divided the components of NPQ dynamics into two groups: short term, ≤30 min (STNPQ), and long term, >30 min (LTNPQ). The

variation measured in both induction and STNPQ relaxation across parental lines of a nested association mapping (NAM) population of soybean was used to assess their value for breeding for increased speeds of adjustment to light fluctuations.

RESULTS

The light absorption of a soybean canopy was simulated for a clear sky (sunny) and intermittently cloudy (cloudy) day in August using the ray-tracing algorithm (Figure 1). The diurnal light absorption for all points in the canopy was simulated over the daylight hours of the sunny (Figure 2a) and the cloudy (Figure 2b) day. At midday on the sunny day, a point on a leaf at the top of the canopy experiences full sunlight (>1000 μmol m^{-2} sec^{-1}) (Figure 2c), whereas all points lower in the canopy experience sun flecks (Figure 2e,g). Sunflecks are seen to be highly dynamic over the course of the day, particularly in the middle layers (Figure 2e). On an intermittently cloudy day, points on both the top leaves and those below are subject to large fluctuations in absorbed light (Figure 2d,f), whereas little light reaches points on the bottom layer (Figure 2f).

The net cumulative canopy assimilation (A_c) was calculated over the daylight hours of the sunny (Figure 3a) and the cloudy (Figure 3b) day, driven by the simulated temporal and spatial dynamics of lighting for the whole canopy. Simulations of A_c compared instantaneous responses to light fluctuations with the slower responses resulting from the delays caused by photosynthetic induction (via Rubisco; Rca), STNPQ (including qE and qM) and LTNPQ. This quantified the loss of potential canopy carbon fixation caused by these delays. On the sunny day, a positive rate of net total carbon assimilation was observed at 07:00 h, and a positive rate of cumulative carbon gain continued until around 18:00 h, when canopy respiration was again predicted to exceed photosynthesis (Figure 3a). Simulated differences in cumulative assimilation resulting from delays in adjustment to light fluctuations become evident around 08:00 h, and progressively amplify in cumulative carbon gain through the daylight hours (Figure 3a). The total loss resulting from these delays is 13.5%, with LTNPQ accounting for the largest part of this loss (Figures 3a and 4). On the cloudy day, because the light intensity was very low in the morning (Figure 2b), the net assimilation was negative from dawn until 09:40 h, because total canopy respiration exceeded the photosynthesis until this time. Beyond this point, the simulated differences in cumulative net assimilation resulting from delays in adjustment to light fluctuations progressively amplified in cumulative net assimilation until 17:00 h (Figure 3b). The total loss as a result of these lags was 12.5%, with STNPQ accounting for the largest part of this loss (Figures 3 and 4). Although the simulated proportionate losses were similar on both days (Figure 4), the absolute loss on the intermittently cloudy day (40 mmol m^{-2}) was less than half that on the sunny day (115 mmol m^{-2}).

Partitioning the causes of simulated losses on the sunny day shows that resulting from LTNPQ was almost twice the loss resulting from STNPQ, and was approximately 2.7 times the loss caused by Rubisco activation (Figure 4). By contrast, on a cloudy day the loss resulting from STNPQ is higher, contributing about 40% of the total loss, whereas the loss resulting from Rubisco induction is similar to that resulting from LTNPQ (Figures 3b and 4).
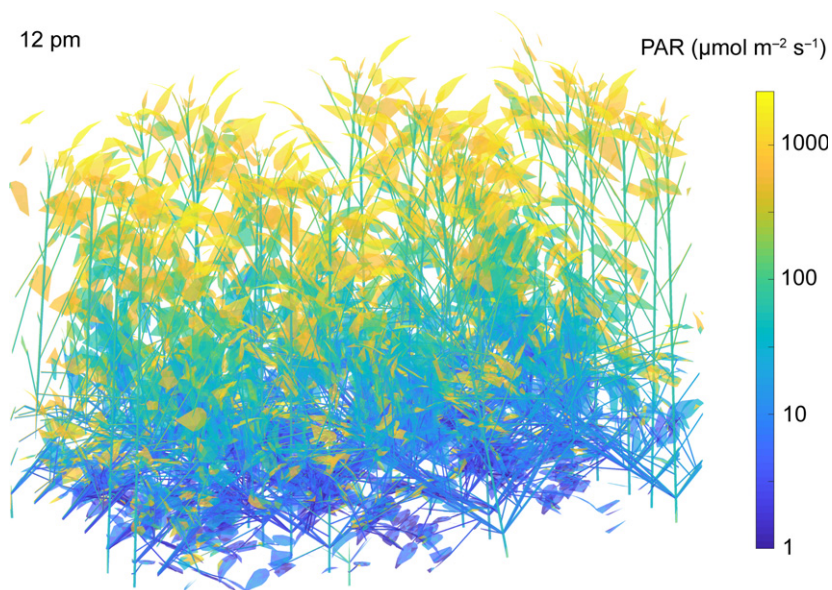

Figure 1. Modelled *Glycine max* (soybean) canopy structure and lighting (PAR = Photosynthetically active photon flux), predicted from ray tracing for a clear sky on 20 August, at Champaign, Illinois, USA (40.11°N). Colors indicate the spatial heterogeneity of the intensity of the absorbed light at noon.
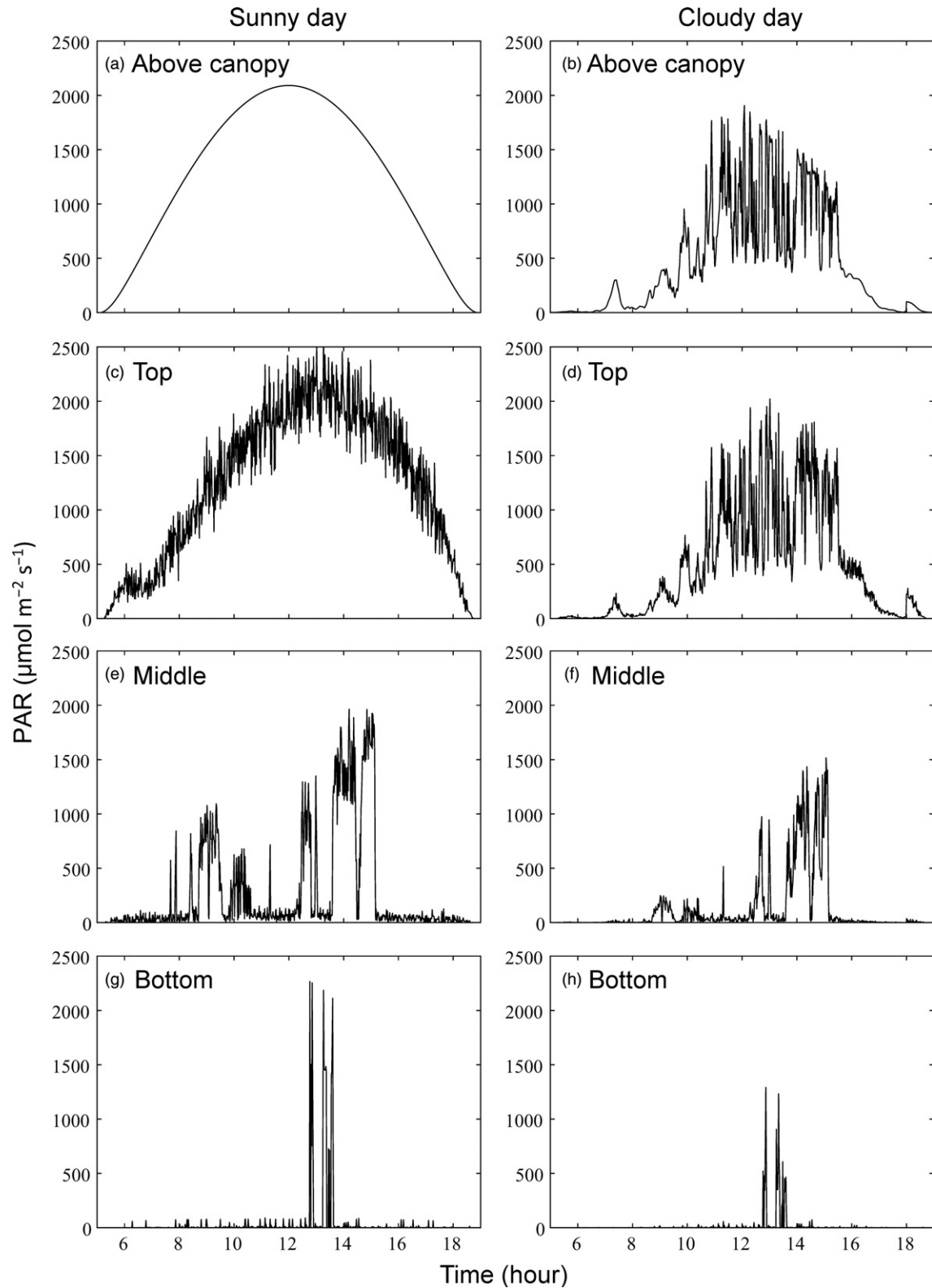
Figure 2. Panel (b) shows the recorded incident photosynthetically active photon flux on 20 August 2019, above the soybean canopy of Figure 1, which was an intermittently cloudy day. Panel (a) shows the predicted light intensity for the same day based on sun–earth geometry and an atmospheric transmittance of 0.85, assuming a cloud-free clear-sky day. The diurnal light absorption simulated for single pixels on the leaves in the top, middle and bottom of the soybean canopy on the sunny day are shown in panels (c), (e) and (g), respectively, and for the cloudy day in panels (d), (f) and (h), respectively.
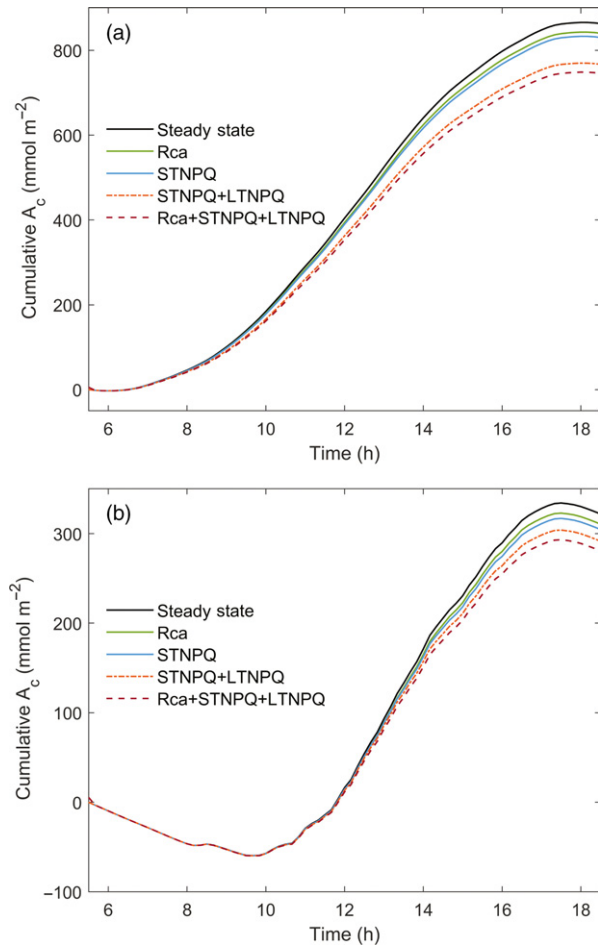
Figure 3. The cumulative net CO_2 assimilation of the *Glycine max* (soybean) canopy of Figure 1 (A_c) on the simulated sunny day (Figure 2a) and actual cloudy day (Figure 2b). The black line is the predicted assimilation of CO_2 that would occur if photosynthesis responded instantaneously to changes in light, with no lags in efficiency. Rca accounts for the losses that result from the lags in the activation of Rubisco on shade–sun transitions. STNPQ accounts for the losses that result from lags in the both forms of NPQ. Rca + STNPQ + LTNPQ accounts for lags in both Rubisco activation and relaxation of NPQ. The simulations starts at dawn (05:30 h), with A_c = 0.
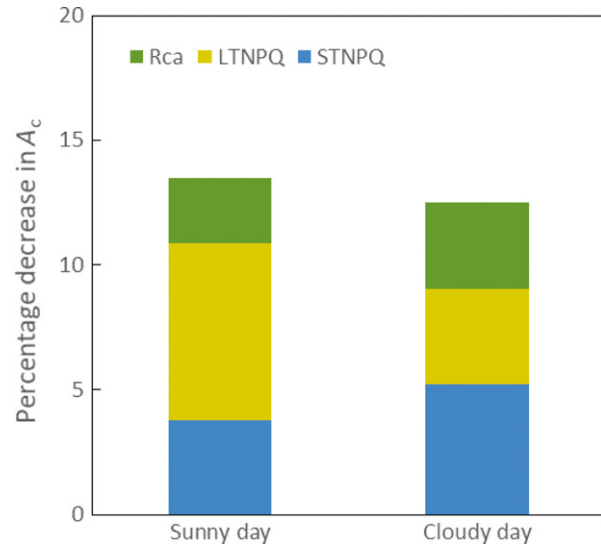

Figure 4. The percentage loss in potential daily canopy photosynthetic net carbon assimilation (A_c) through losses of efficiency from lags in non-photochemical quenching (NPQ) relaxation and Rubisco activation, calculated from the simulation presented in Figure 3. Blue bars (STNPQ) are the decreases in A_c caused by short-term NPQ relaxation; yellow bars (LTNPQ) are the decreases of A_c caused by long-term NPQ relaxation (Zhu *et al.*, 2004); green bars (Rca) are the predicted decreases of A_c resulting from lags in Rubisco activation. The simulated sunny clear-sky day is plotted on the left and the intermittently cloudy day is plotted on the right.

To assess the potential impact of genotypic variation on assimilation, NPQ relaxation rates were measured for the 41 parental lines of the soybean NAM population. Variation in qE and qM across the NAM population were 40 and 49% between the slowest and fastest genotype, respectively. Values for these two genotypes and the average across all members of the NAM population were used in the model. The genotype with the fastest relaxation (NAM27) assimilated about 1.3% more CO_2 across the day compared with the genotype with the slowest relaxation (NAM23), and assimilated approximately 0.8% more CO_2 than average for the sunny day (Figure 5). On the cloudy day, the fastest genotype (NAM27) assimilated approximately 0.9% more

than average (Figure 5), suggesting small but significant additive effects across a growing season.

Previously published measurements of photosynthetic induction in the NAM population showed large variation between genotypes in induction (Soleh *et al.*, 2017). The time course of Rubisco activation ($\tau_{Rubisco}$) for the two genotypes representing the slowest and fastest induction rates, and a third representing the middle of this range, were added here to the canopy model to simulate the variation in loss caused by the speed of the response on the sunny and the cloudy days (Figure 6). The loss in assimilation as a result of Rubisco activation is up to 17.4% for NAM8, which had the slowest Rubisco activation ($\tau_{Rubisco}$ = 1850.0 sec), whereas NAM23, the genotype with the fastest Rubisco activation ($\tau_{Rubisco}$ = 129.7 sec), reduced the loss to only 2.3% on the cloudy day and 1.9% on the sunny day.

DISCUSSION

Using a rendering of an actual fully developed field canopy (Figure 1), the present study suggests that the lower efficiency of photosynthesis during light fluctuations for an elite soybean cultivar costs about 13.5% of potential crop assimilation on both sunny and cloudy days in the critical pod-filling phase (Figure 4). On the simulated clear-sky day, LTNPQ appears to be the largest cause of this loss. On a cloudy day, photosynthetic induction and LTNPQ
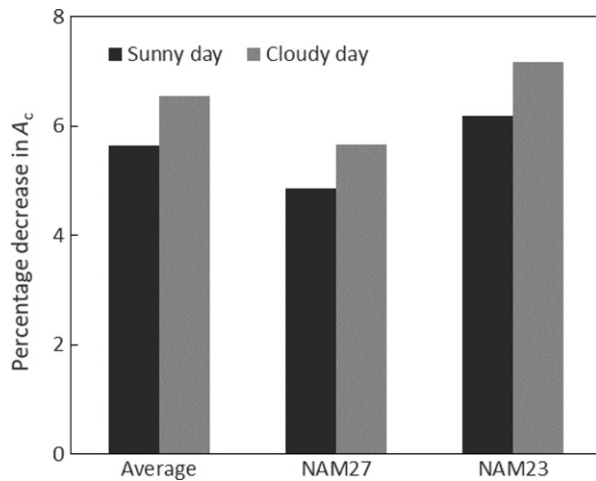
Figure 5. The effect of genetic variation in the speeds of short-term non-photochemical quenching (STNPQ) relaxation on losses of potential daily net CO_2 assimilation (A_c) in the *Glycine max* (soybean) canopy of Figure 1. Illustrated are losses in A_c resulting from the average of the measured rates of relaxation of STNPQ for the nested association mapping (NAM) soybean parent population and for the NAM lines showing the fastest (NAM27) and slowest (NAM23) rates of STNPQ relaxation. Dark-gray bars are losses predicted for the sunny day (Figure 2a) and light-gray bars are losses for the intermittantly cloudy day (Figure 2b).

Figure 6. The effect of genetic variation in the speeds of Rubisco activation on losses of potential daily net CO_2 assimilation (A_c) in the canopy of Figure 1 using the daily sunlight profiles of Figure 2(a, b). Measurements from three *Glycine max* (soybean) genotypes were used (Soleh *et al.,* 2017): NAM23, which showed the fastest activation of Rubisco ($\tau_{Rubisco}$); RC, the average for the population; and NAM8, which showed the slowest activation. Dark-gray bars are losses predicted for the sunny day (Figure 2a) and light-gray bars are losses for the intermittantly cloudy day (Figure 2b).

contribute equally, and the loss resulting from STNPQ contributes the most, at 40% (Figure 4). Crop biomass is about 40% carbon. Assuming then that one mole of CO_2 assimilated, net of respiration, results in 75 g of biomass, then the growth loss resulting from lags in the adjustment of photosynthesis to light fluctuations in the canopy would be a substantial 90 kg ha^{-1} day^{-1} on a sunny day. With no mechanisms known that could allow for the instantaneous induction of photosynthesis on shade–sun transitions or the relaxation of NPQ on sun–shade transitions, it appears unlikely that breeding or bioengineering could recover more than about half of this loss. Nevertheless, a 6.5% increase in net photosynthetic efficiency, if translated into increased crop yields, would be exceptional. It could either provide a key part of the anticipated future need for increased yield potential to ensure global food security or, should food demand stabilize, serve to reduce the global footprint of arable agriculture (Long *et al.,* 2015). How could these losses in fluctuating light be decreased?

The engineered acceleration of STNPQ relaxation has already been undertaken in tobacco by upregulating the levels of the two enzymes involved in the interconversion of violaxanthin and zeaxanthin and the photosystem-II protein PsbS, which affects the amplitude of NPQ. This increased the quantum yield of CO_2 assimilation in fluctuating light and the rate of whole-chain electron transport by approximately 50%. In replicated field trials, biomass production was increased by 14–21%; however, this was achieved with a 50- to 100-fold increase in the two
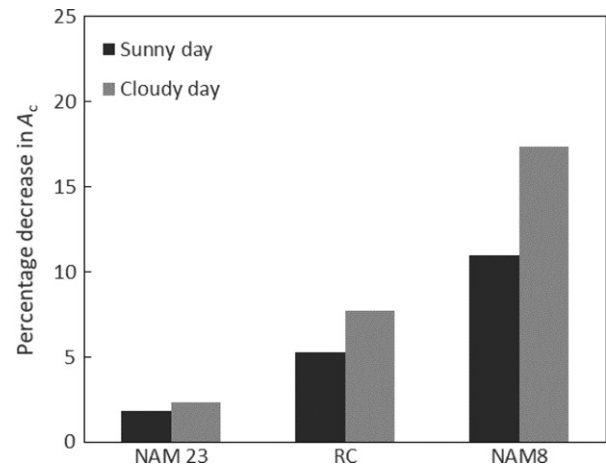
enzymes and an approximately fivefold increase in PsbS (Kromdijk *et al.,* 2016). It would seem unlikely that this scale of diversity exists within the germplasm of a crop, suggesting that improvements on this scale might only be achieved by the transgenic addition of extra copies of the relevant genes or by the engineering of promoter regions to upregulate expression. This might be confirmed by the results obtained here with the NAM population parent lines, where the gain achieved with the fastest STNPQ-relaxing line showed only a 1% improvement over the average in terms of A_c (Figure 5). Although small, this could still have value. In 2017 soybean occupied 124 Mha of the global surface, which produced 353 Mt of beans (FAOStat, 2017). As such, a 0.8% increase could mean an additional 2.8 Mt or it could release over 1 Mha of land no longer needed for soybean production. Importantly, this increase, although small in relative terms, can potentially be gained by conventional breeding.

Given that the relaxation of LTNPQ is the largest contributor to losses on a sunny day, this suggests that the largest gains may be achieved by focusing on this aspect. Several genes, in particular those involved in the repair and replacement of the photosystem-II D1 protein, have been functionally implicated in the slow phase of NPQ recovery (Nixon *et al.,* 2010). Although the optimal targets in crops remain unclear, it will be important to see these tested in model plants. With the rapid growth of complete genomic sequences for many accessions of major crops, genome-wide association analysis provides an approach to reveal further targets (Wang *et al.,* 2017a).

What factors limit the speed of induction on a shade–sun transition? In the chloroplast, photosynthesis is limited by the build-up of Calvin cycle intermediates, in particular the CO_2 acceptor molecule ribulose 1,5-bisphoshate, and the induction of light-activated photosynthetic enzymes, in particular the activation of Rubisco by Rca. Sufficient accumulation of ribulose 1,5-bisphoshate is assumed to require approximately 60 sec, whereas the activation of Rubisco may require more than 10 min (Mott and Woodrow, 2000; Taylor and Long, 2017). At the leaf level, induction can be limited by slow stomatal opening, where full opening can require many minutes (McAusland *et al.*, 2016; De Souza *et al.*, 2019; Faralli *et al.*, 2019; Acevedo-Siaca *et al.*, 2020), and by mesophyll conductance, which generally increases with incident light. The rate of increase in mesophyll conductance upon induction is generally considered faster than both stomatal opening and Rubisco activation (Deans *et al.*, 2019), but the variability between species and environmental conditions is not well defined. Several studies have inferred from both modeling and the *in vivo* estimation of Rubisco activity ($V_{c,max}$) that the activation of Rubisco is the key limitation to the speed of induction (Mott and Woodrow, 2000; Yamori *et al.*, 2012; Soleh *et al.*, 2016; Soleh *et al.*, 2017; Taylor and Long, 2017). This gains support from the observation that in wheat and soybean, intercellular [CO_2] is higher during induction than at steady state (Soleh *et al.*, 2017; Taylor and Long, 2017), whereas the converse would be expected if stomatal opening was the dominant factor. In other species the speed of stomatal opening appears to be the dominant limitation limiting the speed of induction (McAusland *et al.*, 2016; De Souza *et al.*, 2019), and this may be accentuated under stress conditions (Faralli *et al.*, 2019). In the current study, only the activation of Rubisco by Rca was considered, so the losses resulting from slow induction must be considered a minimum, where slow increases in stomatal and mesophyll conductance could exacerbate these losses. There is already evidence that increasing the activity of Rca by the upregulation of expression increases the speed of activation (Yamori *et al.*, 2012), whereas site-directed mutagenesis has been shown as a non-transgenic means to increase Rca activity (Perdomo *et al.*, 2019). In addition, significant natural variation in the speed of induction has been demonstrated within the germplasm of cassava, soybean and wheat (Soleh *et al.*, 2017; De Souza *et al.*, 2019; Salter *et al.*, 2019), providing further non-transgenic opportunities for decreasing the losses resulting from reduced photosynthetic efficiency during induction. Simulation of this variation in our canopy model suggests that considerable gains could be achieved in soybean by conventional breeding that selects for faster rates of induction (Figure 6).

The purpose of this work was to highlight the potential for improving crop photosynthesis under non-steady-state lighting conditions. To do this we had to draw on disparate sources for model parameterization, as not all parameters were available for soybean. Additionally, some of the parameters used were measured using different protocols, such as NPQ relaxation kinetics of soybean cv. LD11-2170 and the NAM population. Therefore, the predictions here should be taken only as an indication of opportunity, and need to be further improved by better measurements and parametrization. First, the rate constant of the NPQ relaxation is possibly related to light intensities or light-intensity differences (Dall'Osto *et al.*, 2014). Second, it is not clear how leaf position and age influence the NPQ relaxation speed. Third, the long-term NPQ responses of soybean and most major crops have not been well defined, and the correlation between LTNPQ and the accumulated light input has not been validated with sufficient data. Fourth, the correlation between Rubisco activation kinetics and light intensity is poorly defined. Thus more integrated measurement and analysis of NPQ relaxation, Rubisco activation kinetics, stomatal opening and mesophyll conductance dynamics in the major crops will improve the model prediction and ability to partition causes. Finally, the lighting was simulated for 5-mm^2 pixels of the leaf surface; however, NPQ activation and Rubisco activation occur at the level of the chloroplast, with a cross-sectional area of about 25 μm^2. As a result, the speed of the light change at an individual chloroplast with the change in solar angle will be faster than that simulated. Simulating smaller areas greatly increases the computational time, but is likely to become practical as computational power increases. The compromise used here will have resulted in some underestimation of the cost of these light transitions, however.

In conclusion, this first model analysis of light fluctuations in a rendering of an actual crop canopy indicates unexploited breeding and bioengineering targets to substantially improve photosynthetic efficiency and productivity. Although this analysis is limited to soybean, it appears reasonable to expect similar gains in other C3 crops, including cassava, wheat and rice. Although we cannot be certain that an improvement in photosynthetic efficiency will increase the yield, there is evidence for all four crops that an artificial increase in leaf photosynthesis by season-long elevation of [CO_2] under open-air field conditions results in highly significant increases in yield (Long *et al.*, 2006; Rosenthal *et al.*, 2012; Hasegawa *et al.*, 2013).

EXPERIMENTAL PROCEDURES

3D soybean model and light distribution simulations

The dynamics of lighting within a soybean canopy were predicted with a 3D architectural representation, using our previously presented framework for crop canopies (Song *et al.*, 2013; Wang *et al.*, 2017b). The model was parameterized on the measured architecture of a soybean crop (*G. max* L. Merr., Pioneer 93B15) on the University of Illinois South Farms. The leaf lengths, widths, petiole lengths

and angles for trifoliate leaves of soybean (Aug 20) were obtained from Song *et al.*, (2019). The canopy had a row spacing of 38 cm and a plant spacing within the rows of 10 cm. The model divides the surface of each leaf into 'pixels' of approximately 5 mm^2 in area, which is much smaller than the 'pixels' used in Song *et al.*, (2019; about 1 cm^2). To estimate light changes in the canopy, a forward ray-tracing algorithm (FASTTRACER; Song *et al.*, 2013; Wang *et al.*, 2017b; Townsend *et al.*, 2018; Song *et al.*, 2019) was used to predict the light absorption of each 5-mm^2 pixel every 10 sec from 05:00 to 19:00 h on 20 August 2019 in Champaign, IL, USA (40.11 N, 88.21 W). At each time point the direct and diffuse light entering and within the canopy is predicted, together with the scattered radiation through reflection from, and transmission through, the leaves within the canopy. Leaf reflectance and transmission were both set to 0.075 (Song *et al.*, 2013). The sum of the direct, diffuse and scattered light incident at each pixel, less the reflectance and transmission, gave the absorbed photosynthetically active photon flux. Atmospheric transmittance was set as 0.85 to estimate the incident direct and diffuse light reaching the top of the canopy at each time point on a sunny day (Song *et al.*, 2013). A partially cloudy day was simulated by using the measured direct and diffuse light on 20 August 2018 in Bondville, IL, USA (SURFRAD, 2019). For each time point (*t*), the light absorption of each 5-mm^2 leaf pixel on the cloudy day, $I_{l\_c}(t)$, was calculated as:

$$I_{l\_c}(t) = I_{l\_s}(t)\frac{Q_{in\_c}(t)}{Q_{in\_s}(t)}, \tag{1}$$

where $I_{l\_s}(t)$ is the light absorption of each leaf pixel on the sunny day, which was calculated by the ray-tracing algorithm. $Q_{in\_s}(t)$ is the incident light above the canopy on the sunny day and $Q_{in\_c}(t)$ is the incident light above the canopy on the cloudy day, based on the actual incident light measured.

Simulation of dynamic photosynthesis

Dynamic photosynthetic rates were calculated for every 10 sec (Δt) of the day using the absorbed light for each 5-mm^2 pixel, considering the rates of Rubisco activation and NPQ relaxation. Rubisco deactivation was also taken into account, as the extent of the deactivation during a period of shade affects the duration of the induction following a return to higher light levels. The *in vivo* dynamics of Rubisco activation were calculated using the Rca model of Mott and Woodrow (2000). The steady-state maximum Rubisco activity (V_{cmax0_s}) was related to the level of Rca (70 mg m^{-2}) (Mott and Woodrow, 2000), where K_{aRca} is a constant in determining the maximum steady-state activity of Rubisco (Table 1):

$$V_{c\max0\_s} = \frac{V_{c\max0}[\text{Rca}]}{k_{a_{Rca}} + [\text{Rca}]} \tag{2}$$

The maximum Rubisco activity (V_{cmax}) was calculated by the following equations:

$$V_{\max\_s}(t) = V_{c\max0\_s}\frac{I_l(t)}{k_{\text{light}} + I_l(t)}, \tag{3}$$

$$A_{v\max}(t) = A_{v\max}(t-\Delta t) - \Delta t \cdot \frac{(A_{v\max}(t-\Delta t) - V_{\max\_s}(t))}{\tau_{\text{Rubisco}}}, \tag{4}$$

$$V_{c\max}(t) = A_{v\max}(t) \cdot V_{c\max\_0}, \tag{5}$$

where *t* is time (s), $I_l(t)$ is the absorbed light of each leaf unit at time *t* and K_{light} are constants (Table 1). τ_{Rubisco} is the time constant of Rubisco activation and deactivation; here, τ_{Rubisco} is

180 sec for Rubisco activation and 300 sec for Rubisco deactivation (Taylor and Long, 2017). $A_{v\max}(t)$ is the activated proportion of Rubisco.

The short-term relaxation kinetics of non-photochemical quenching (STNPQ) was defined as the dynamics of NPQ relaxation over the first 30 min, and is described by a bi-exponential curve (Dall'Osto *et al.*, 2014). Here, qE is the fast relaxing energy-dependent quenching, whereas qM combines all of the remaining processes up to 30 min:

$$\Phi_{\text{NPQs}}(t) = N_1 I_l(t) + N_0 \tag{6}$$

$$\Phi_{qE}(t) = \Phi_{qE}(t-\Delta t) - \Delta t \cdot \frac{(\Phi_{qE}(t-\Delta t) - \Phi_{\text{NPQs}}(t) \cdot P_{qE})}{\tau_{qE}} \tag{7}$$

$$\Phi_{qM}(t) = \Phi_{qM}(t-\Delta t) - \Delta t \cdot \frac{(\Phi_{qM}(t-\Delta t) - \Phi_{\text{NPQs}}(t) \cdot P_{qM})}{\tau_{qM}} \tag{8}$$

$$\Phi_{\text{NPQ}}(t) = \Phi_{qE}(t) + \Phi_{qM}(t) \tag{9}$$

where Φ_{NPQs} is the steady state Φ_{NPQ} obtained from the measured light-response curves (see next section) of soybean (cv. LD11-2170). N_1 and N_0, which are set to 0.00028 and 0.0371, are constants calculated from the measured Φ_{NPQs}. P_{qE} and P_{qM} are the proportions of qE and qM. τ_{qE} and τ_{qM} are the time constants of qE and qM relaxation, respectively.

Long-term non-photochemical quenching (LTNPQ), which includes, among other terms, photoinhibitory quenching (qI) and photoinhibition-independent sustained quenching (qH) decreases the maximum quantum yield of photosystem II (PSII) and in turn the maximum quantum yield of CO$_2$ uptake (Zhu *et al.*, 2004). Following Zhu *et al.* (2004), the LTNPQ was correlated with a weighted light dose, and the change in the maximum quantum yield of PSII photochemistry, $A_{Fv/Fm}(t)$, was calculated as:

$$T_f = 0.0033T^2 - 0.1795T + 3.4257, \tag{10}$$

$$I_{\text{int}}(t) = \sum_{i=1}^{i=60} \frac{I_l(t-i)}{\left(1 - \frac{i-1}{60}\right)}, \tag{11}$$

$$A_{Fv/Fm}(t) = 1 - I_{\text{int}}(t) \cdot \frac{T_f}{f_h}, \tag{12}$$

where I_{int} is the weighted light dose at time t. T_f is an empirical factor relating the relative decrease of *Fv/Fm* to temperature (*T*), and *T* was set as 25°C. f_h is an empirical constant used in determining the decrease of *Fv/Fm* for a given I_{int}. For cold-susceptible species, f_h is 5.13.

The quantum yield of PSII was calculated as:

$$\Phi_{\text{PSII}} = A_{Fv/Fm}(t) \cdot Fv/Fm - \Phi_{\text{NPQ}}(t). \tag{13}$$

The electron transport rate, and in turn the rate of leaf CO$_2$ uptake (*A*), is limited by the quantum yield of PSII, incident light and maximum electron transport capacity ($J_{\max}$):

$$J = \min\left(\frac{1}{2}\Phi_{\text{PSII}}I(t), J_{\max}\right). \tag{14}$$

The rate of leaf CO$_2$ uptake (*A*) at time *t* was simulated by the following equations:

$$A_j(t) = \frac{(C_i - \Gamma^*)J(t)}{(4C_i + 9.3\Gamma^*)} - R_d, \tag{15}$$

Table 1 Input parameters of the *Glycine max* (soybean) canopy model

Parameter	Full name	Value	Reference
C_i	Intercellular CO_2 concentration	280 μbar	Environmental input
f_h	Empirical constant in determining the decrease of F_v/F_m for a given I_{int}.	5.1e+5	Zhu *et al.* (2004)
Fv/Fm	Maximum quantum yield of photosystem II	0.801	Measured
Γ^*	The CO_2 compensation point in the absence of dark respiration	38.6 μbar	Von Caemmerer (2000)
J_{max}	Maximum electron transport capacity	200 μmol m^{-2} sec^{-1}	Bernacchi *et al.* (2005)
K_o	Michaelis–Menten constant of Rubisco for O_2	404 mbar	Von Caemmerer (2000)
K_c	Michaelis–Menten constant of Rubisco for CO_2	248 μbar	Von Caemmerer (2000)
k_{aRac}	A constant for the calculation of maximum steady-state Rubisco activity (eqn 2)	12.4 mg m^{-2}	Mott and Woodrow (2000)
k_{light}	A constant for the calculation of steady-state Rubisco activity (eqn 3)	120 μmol m^{-2} sec^{-1}	Sage and Seemann (1993)
K_{TaoRac}	A constant for the calculation of the time constant of Rubisco activation	214 min mg m^{-2}	Mott and Woodrow (2000), Soleh *et al.* (2016)
O_2	Intercellular O_2 concentration	210 mbar	Environmental input
PqE	Proportion of the contribution of qE in steady-state ΦNPQ	0.7	Measured
PqM	Proportion of the contribution of qM in steady-state ΦNPQ	0.3	Measured
[Rac]	Concentration of Rubisco activase	70 mg m^{-2}	Mott and Woodrow (2000)
R_{d0}	Dark respiration	1.2 μmol m^{-2} sec^{-1}	Measured
Temp	Leaf temperature	25°C	Environmental input
τ_{qE}	Time constant of qE relaxation	0.56 min	Measured
τ_{qM}	Time constant of qM relaxation	16.8 min	Measured
V_{max0}	Maximum Rubisco activity	120 μmol m^{-2} sec^{-1}	Bernacchi *et al.* (2005)

Table 2 Measured non-photochemical quenching (NPQ) relaxation parameters of *Glycine max* (soybean) cv. LD11-2170

Parameters	Soybean
F_v/F_m	0.801 ± 0.032
Φ_{qE}	0.318 ± 0.016
Φ_{qI}	0.097 ± 0.015
Φ_{qM}	0.066 ± 0.008
τ_{qE} (min)	0.558 ± 0.051
τ_{qM} (min)	16.826 ± 9.134

$$A_c(t) = \frac{V_{c\max}(t)(C_i - \Gamma^*)}{\left(C_i + K_c\left(1 + \frac{O_2}{K_o}\right)\right)} - R_d, \tag{16}$$

$$A(t) = \min(A_j(t), A_c(t)), \tag{17}$$

where R_d is the leaf respiration. As lower canopy leaves respire less than upper canopy leaves, R_d was scaled with the overlying leaf area index (LAI), as described previously (Srinivasan *et al.*, 2017):

$$R_d(z) = R_{d0} \exp(-kn \cdot LAI(z)), \tag{18}$$

where R_{d0} is the respiration of the uppermost leaf layer with a measured value of 1.2 (± 0.22) for soybean (cv. LD11-2170) and kn is an exponential extinction coefficient with a measured value of 0.2 (Srinivasan *et al.*, 2017).

Then the canopy net CO_2 uptake (A_c) was calculated as:

$$A_c(t) = \frac{\sum(A_i(t) \cdot S_i)}{S_{ground}}, \tag{19}$$

where $A_i(t)$ is the CO_2 uptake rate of a leaf pixel, S_i is the surface area of each pixel and S_{ground} represents the occupied ground area of the simulated canopy. All simulations were conducted in MATLAB 2017 (Mathworks®, https://uk.mathworks.com).

Measurement of dynamic NPQ parameters

To determine the kinetics of STNPQ relaxation in soybean (parameters listed in Table 2), chlorophyll fluorescence and gas exchange were measured during the transition from high light (1800 μmol m^{-2} sec^{-1}) to low light (200 μmol m^{-2} sec^{-1}). Measurements were taken on 9 March 2019 in a controlled-environment glasshouse at the University of Illinois at Urbana-Champaign. The air temperature inside the glasshouse was set as 28°C (day)/24°C (night). Leaf CO_2 uptake and modulated chlorophyll fluorescence of the youngest fully expanded leaf was measured on 30-day-old soybean plants (cv. LD11-2170) with a gas-exchange system incorporating a controlled-environment leaf cuvette with a head containing a modulated chlorophyll fluorometer and an LED light source (LI-6400XT and LI-6400-40; LI-COR, https://www.licor.com). The measurements were made on six replicate plants. The leaves were first acclimated to dark for 30 min, with a leaf cuvette temperature (T_{block}) of 28°C and a [CO_2] of 400 μmol mol^{-1}; the light intensity was then increased to 1800 μmol m^{-2} sec^{-1} for 30 min and then decreased to 200 μmol m^{-2} sec^{-1} for the next 30 min, to simulate a sun–shade transition. Leaf CO_2 exchange and modulated chlorophyll fluorescence were recorded before the light was turned on, and then every 60 sec for the following 30 min. The measured time series data of ΦNPQ changes, represented by the following equation (Dall'Osto *et al.*, 2014):

$$\Phi_{NPQ} = \Phi_{qI} + \Phi_{qE}e^{(-t/\tau qE)} + \Phi_{qM}e^{(-t/\tau qM)}, \qquad (20)$$

were fitted with a polynomial (fit function; MATLAB 2017). The fitted values are listed in Table 2.

For light-response curves, the leaf was dark-adapted for 30 min and then acclimated to a light intensity of 1500 µmol m^{-2} sec^{-1} and a CO_2 concentration of 400 µmol mol^{-1} inside the cuvette. After 20 min the chamber light was varied according to the following sequence: 2000, 1500, 1000, 500, 300, 200, 100 and 50 µmol m^{-2} sec^{-1}. Chlorophyll fluorescence and gas-exchange measurements were recorded after the conditions inside the cuvette regained stability at each light level, the minimal time interval was 5 min. Chlorophyll fluorescence measurements were used to calculate steady-state NPQ (Φ_{NPQs}, eqn 6).

Variation in the rate of recovery of STNPQ quenching across the parents of the soybean NAM population

The 41 parents of the soybean NAM population (Song *et al.*, 2017; Diers *et al.*, 2018) were planted on the South Farms of the University of Illinois at Urbana-Champaign, on 6 June 2019. The parents were planted in 1.2-m-long single-row plots with a 0.75-m row spacing. The experiment was arranged with a randomized complete block design with five replicate plots per genotype. On the 26 July 2019, when plants were at the R1 developmental stage, three 0.48-mm leaf disks were collected from the uppermost mature leaf of each replicate plot in the field and floated on water in 24-well plates for transport back to the laboratory. Leaf disks were then laid adaxial side up on square Petri dishes containing damp filter paper, sealed, wrapped in aluminum foil and incubated overnight at 25°C to allow for the complete relaxation of NPQ. The next day, the modulated PSII chlorophyll fluorescence of the disks on each Petri dish was imaged (FluorCam FC 800-C; PSI-Photon Systems Instruments, Drasov, Czech Republic, https://psi.cz/). Disks were exposed to 10 min of approximately 1000 µmol m^{-2} sec^{-1} white light (6500 K) to induce NPQ and then 50 min of darkness. Saturating pulses (4000 µmol m^{-2} sec^{-1} white light) to determine F_m were given at 9, 40, 60, 80, 100, 120, 160, 200, 240, 300, 360, 420, 480, 540 and 598 sec after the actinic light was turned on, and at 1, 2, 4, 6, 8, 10, 14, 18, 22, 26, 32, 38, 44 and 50 min after the actinic light was turned off. The background was excluded automatically and NPQ values at each pulse were calculated. The maximum NPQ value for each leaf disk was set to 1, with other values normalized relative to this. Relaxation of NPQ with time was fitted by nonlinear least squares to equation 19 (nls function, R-project).

Simulating the effect of variation in photosynthetic induction across the NAM parent lines

Measured time courses of Rubisco (V_{cmax}) activation during photosynthetic induction were extracted from Soleh *et al.* (2017) for the NAM parent lines, using image-capture and analysis software (GETDATA GRAPH DIGITIZER, obtained from S. Federov, http://getdata-graph-digitizer.com). Fifteen points were captured per curve for each leaf disk and then fitted to an exponential function:

$$V_{c\,max} = ae^{(-t/\tau_{Rubisco})} + c, \qquad (20)$$

where $\tau_{Rubisco}$ is the time constant of Rubisco activation, c is the Rubisco activity in the dark and a is the increase of Rubisco activity from dark to light. The fitted values are listed in Table 3. Then the measured $\tau_{Rubisco}$ values for NAM23, RC and NAM8 were used in this simulation. The time constant of Rubisco deactivation was assumed to be double the time required for the activation of each genotype (Taylor and Long, 2017).

Table 3 Rubisco activation parameters estimated by using the time course of maximum carboxylation capacity of three selected parents of the *Glycine max* (soybean) nested association mapping (NAM) population during the induction response (Soleh *et al.*, 2017)

Parameters	NAM23	RC	NAM8
a (µmol m^{-2} sec^{-1})	72.2	80.0	85.0
c (µmol m^{-2} sec^{-1})	21.6	17.3	7.6
$\tau_{Rubisco}$ (sec)	129.7	471.7	1850.0
R^2	0.982	0.977	0.976

AUTHOR CONTRIBUTIONS

SPL, YW and SJB designed the study. YW performed the computational analysis. YW, EMDB and SJB conducted the STNPQ measurements. SPL, YW, SJB and EMDB wrote the article.

CONFLICT OF INTEREST

The authors declare that they have no conflicts of interest.

DATA AVAILABILITY STATEMENT

The code and data are available at https://doi.org/10.13012/B2IDB-9453481_V1.

REFERENCES

Acevedo-Siaca, L.G., Coe, R., Wang, Y., Kromdijk, W., Quick, W.P. and Long, S.P. (2020) Variation in photosynthetic induction between rice accessions and its potential for improving productivity. *New Phytol.* accepted.

Bernacchi, C.J., Morgan, P.B., Ort, D.R. and Long, S.P. (2005) The growth of soybean under free air [CO 2] enrichment (FACE) stimulates photosynthesis while decreasing in vivo Rubisco capacity. *Planta*, **220**, 434–446.

Cazzaniga, S., Osto, L.D., Kong, S.G., Wada, M. and Bassi, R. (2013) Interaction between avoidance of photon absorption, excess energy dissipation and zeaxanthin synthesis against photooxidative stress in Arabidopsis. *Plant Journal*, **76**, 568–579.

Dall'Osto, L., Caffarri, S. and Bassi, R. (2005) A mechanism of nonphotochemical energy dissipation, independent from PsbS, revealed by a conformational change in the antenna protein CP26. *Plant Cell*, **17**, 1217–1232.

Dall'Osto, L., Cazzaniga, S., Wada, M. and Bassi, R. (2014) On the origin of a slowly reversible fluorescence decay component in the Arabidopsis npq4 mutant. *Philos. Trans. R. Soc. Lond. B. Biol. Sci.* **369**, 20130221.

De Souza, A.P., Wang, Y., Orr, D.J., Carmo-Silva, E. and Long, S.P. (2019) Photosynthesis across African cassava germplasm is limited by Rubisco and mesophyll conductance at steady-state, but by stomatal conductance in fluctuating light. *New Phytol.* https://doi.org/10.1111/nph.16142

Deans, R.M., Farquhar, G.D. and Busch, F.A. (2019) Estimating stomatal and biochemical limitations during photosynthetic induction. *Plant Cell Environ.* **42**, 3227–3240.

Diers, B.W., Specht, J., Rainey, K.M., Cregan, P., Song, Q., Ramasubramanian, V., Graef, G., Nelson, R., Schapaugh, W. and Wang, D. (2018) Genetic architecture of soybean yield and agronomic traits. *G3: Genes - Genomes - Genetics*, **8**, 3367–3375.

Dunstone, R.L., Gifford, R.M. and Evans, L.T. (1973) Photosynthetic characteristics of modern and primitive wheat species in relation to ontogeny and adaptation to light. *Aust. J. Biol. Sci.*, **26**, 295–307.

FAOStat. (2017) *FAOSTAT*. Rome, Italy: Food and Agriculture Organization of the United Nations.

Faralli, M., Cockram, J., Ober, E., Wall, S., Galle, A., Van Rie, J., Raines, C. and Lawson, T. (2019) Genotypic, developmental and environmental effects on the rapidity of g(s) in wheat: impacts on carbon gain and water-use efficiency. *Front Plant. Sci.* **10**, https://doi.org/10.3389/fpls.2019.00492.

Hasegawa, T., Sakai, H., Tokida, T. *et al.* (2013) Rice cultivar responses to elevated CO2 at two free-air CO2 enrichment (FACE) sites in Japan. *Funct. Plant Biol.* **40**, 148–159.

Köhler, I.H., Ruiz-Vera, U.M., VanLoocke, A., Thomey, M.L., Clemente, T., Long, S.P., Ort, D.R. and Bernacchi, C.J. (2016) Expression of cyanobacterial FBP/SBPase in soybean prevents yield depression under future climate conditions. *J. Exp. Bot.* **68**, 715–726.

Krause, G.H., Vernotte, C. and Briantais, J.M. (1982) Photoinduced quenching of chlorophyll fluorescence in intact chloroplasts and algae - resolution into 2 components. *Biochim Biophys Acta.* **679**, 116–124.

Kromdijk, J., Glowacka, K., Leonelli, L., Gabilly, S.T., Iwai, M., Niyogi, K.K. and Long, S.P. (2016) Improving photosynthesis and crop productivity by accelerating recovery from photoprotection. *Science*, **354**, 857–861.

Long, S.P., Ainsworth, E.A., Rogers, A. and Ort, D.R. (2004) Rising atmospheric carbon dioxide: Plants face the future. *Annu. Rev. Plant Biol.* **55**, 591–628.

Long, S.P., Ainsworth, E.A., Leakey, A.D.B., Nosberger, J. and Ort, D.R. (2006) Food for thought: lower-than-expected crop yield stimulation with rising CO2 concentrations. *Science*, **312**, 1918–1921.

Long, S.P., Marshall-Colon, A. and Zhu, X.G. (2015) Meeting the global food demand of the future by engineering crop photosynthesis for yield potential. *Cell*, **161**, 56–66.

Malnoe, A., Schultink, A., Shahrasbi, S., Rumeau, D., Havaux, M. and Niyogi, K.K. (2018) The plastid lipocalin LCNP is required for sustained photoprotective energy dissipation in Arabidopsis. *Plant Cell*, **30**, 196–208.

McAusland, L., Vialet-Chabrand, S., Davey, P., Baker, N.R., Brendel, O. and Lawson, T. (2016) Effects of kinetics of light-induced stomatal responses on photosynthesis and water-use efficiency. *New Phytol.* **211**, 1209–1220.

Mott, K.A. and Woodrow, I.E. (2000) Modelling the role of Rubisco activase in limiting non-steady-state photosynthesis. *J. Exp. Bot.* **51**, 399–406.

Nilkens, M., Kress, E., Lambrev, P., Miloslavina, Y., Muller, M., Holzwarth, A.R. and Jahns, P. (2010) Identification of a slowly inducible zeaxanthin-dependent component of non-photochemical quenching of chlorophyll fluorescence generated under steady-state conditions in Arabidopsis. *BBA-Bioenergetics*, **1797**, 466–475.

Nixon, P.J., Michoux, F., Yu, J.F., Boehm, M. and Komenda, J. (2010) Recent advances in understanding the assembly and repair of photosystem II. *Ann. Bot.* **106**, 1–16.

Perdomo, J.A., Degen, G.E., Worrall, D. and Carmo-Silva, E. (2019) Rubisco activation by wheat Rubisco activase isoform 2β is insensitive to inhibition by ADP. *Biochem J.* **476**, 2595–2606.

Pignon, C.P., Jaiswal, D., McGrath, J.M. and Long, S.P. (2017) Loss of photosynthetic efficiency in the shade. An Achilles heel for the dense modern stands of our most productive C-4 crops? *J. Exp. Bot.* **68**, 335–345.

Rawson, H.M., Hindmarsh, J.H., Fischer, R.A. and Stockman, Y.M. (1983) Changes in leaf photosynthesis with plant ontogeny and relationships with yield per ear in wheat cultivars and 120-progeny. *Aust. J. Plant Physiol.* **10**, 503–514.

Rosenthal, D.M., Slattery, R.A., Miller, R.E., Grennan, A.K., Cavagnaro, T.R., Fauquet, C.M., Gleadow, R.M. and Ort, D.R. (2012) Cassava about-FACE: greater than expected yield stimulation of cassava (Manihot esculenta) by future CO2 levels. *Glob. Change Biol.* **18**, 2661–2675.

Sage, R.F. and Seemann, J.R. (1993) Regulation of ribulose-1, 5-bisphosphate carboxylase/oxygenase activity in response to reduced light intensity in C4 plants. *Plant Physiol.* **102**, 21–28.

Salter, W.T., Merchant, A.M., Richards, R.A., Trethowan, R. and Buckley, T.N. (2019) Rate of photosynthetic induction in fluctuating light varies widely among genotypes of wheat. *J. Exp. Bot.* **70**, 2787–2796.

Sinclair, T.R., Rufty, T.W. and Lewis, R.S. (2019) Increasing photosynthesis: unlikely solution for world food problem. *Trends Plant Sci.* **24**, 1032–1039.

Soleh, M.A., Tanaka, Y., Nomoto, Y., Iwahashi, Y., Nakashima, K., Fukuda, Y., Long, S.P. and Shiraiwa, T. (2016) Factors underlying genotypic differences in the induction of photosynthesis in soybean [Glycine max (L.) Merr.]. *Plant Cell Environ.* **39**, 685–693.

Soleh, M.A., Tanaka, Y., Kim, S.Y., Huber, S.C., Sakoda, K. and Shiraiwa, T. (2017) Identification of large variation in the photosynthetic induction response among 37 soybean Glycine max (L.) Merr. genotypes that is not correlated with steady-state photosynthetic capacity. *Photosynth. Res.* **131**, 305–315.

Song, Q.F., Zhang, G.L. and Zhu, X.G. (2013) Optimal crop canopy architecture to maximise canopy photosynthetic CO2 uptake under elevated CO2 - a theoretical study using a mechanistic model of canopy photosynthesis. *Funct. Plant Biol.* **40**, 109–124.

Song, Q., Yan, L., Quigley, C. *et al.* (2017) Genetic characterization of the soybean nested association mapping population. *Plant Genome*, **10**(2), 1–14. https://doi.org/10.3835/plantgenome2016.10.0109

Song, Q., Srinivasan, V., Long, S.P. and Zhu, X.-G. (2019) Decomposition analysis on soybean productivity increase under elevated CO2 using 3D canopy model reveals synergestic effects of CO2 and light in photosynthesis. *Ann. Bot.* pii:mcz163. https://doi.org/10.1093/aob/mcz163

South, P.F., Cavanagh, A.P., Liu, H.W. and Ort, D.R. (2019) Synthetic glycolate metabolism pathways stimulate crop growth and productivity in the field. *Science*, **363**, pii: eaat9077.

SURFRAD (2019) Radiation Data Plots: Earth System Research Laboratory, Global Monitoring Division, National Oceanic & Atmospheric Administration, Department of Commerce, USA.

Tanaka, Y., Adachi, S. and Yamori, W. (2019) Natural genetic variation of the photosynthetic induction response to fluctuating light environment. *Curr. Opin. Plant Biol.* **49**, 52–59.

Taylor, S.H. and Long, S.P. (2017) Slow induction of photosynthesis on shade to sun transitions in wheat may cost at least 21% of productivity. *Philos. Trans. R. Soc. Lond. B. Biol. Sci.* **372**, pii: 20160543.

Townsend, A.J., Retkute, R., Chinnathambi, K., Randall, J.W., Foulkes, J., Carmo-Silva, E. and Murchie, E.H. (2018) Suboptimal acclimation of photosynthesis to light in wheat canopies. *Plant Physiol.* **176**, 1233–1246.

Von Caemmerer, S. (2000) *Biochemical Models of Leaf Photosynthesis*. Clayton Vic.: CSIRO Publishing.

Wang, Q.X., Zhao, H., Jiang, J.P., Xu, J.Y., Xie, W.B., Fu, X.K., Liu, C., He, Y.Q. and Wang, G.W. (2017a) Genetic architecture of natural variation in rice nonphotochemical quenching capacity revealed by genome-wide association study. *Front. Plant Sci.* **8**, 1773.

Wang, Y., Song, Q.F., Jaiswal, D., de Souza, A.P., Long, S.P. and Zhu, X.G. (2017b) Development of a Three-dimensional ray-tracing model of sugarcane canopy photosynthesis and its application in assessing impacts of varied row spacing. *Bioenergy Res.* **10**, 626–634.

Winer, J. (2019) Looking in the wrong direction for higher-yielding crop genotypes. *Trends Plant Sci.* **24**, 927–933.

Yamori, W., Masumoto, C., Fukayama, H. and Makino, A. (2012) Rubisco activase is a key regulator of non-steady-state photosynthesis at any leaf temperature and to a lesser extent, of steady-state photosynthesis at high temperature. *Plant J.* **71**, 871–880.

Zhu, X.G., Ort, D.R., Whitmarsh, J. and Long, S.P. (2004) The slow reversibility of photosystem II thermal energy dissipation on transfer from high to low light may cause large losses in carbon gain by crop canopies: a theoretical analysis. *J. Exp. Bot.* **55**, 1167–1175.